(^{3}1). The P–N bonds lengthen by 4 pm in going from ^{1}3 to ^{3}3 and the nitrogens remain slightly pyramidal.

At the correlated MP-2 level, ^{1}1 is lower in energy than ^{3}1 by 8.7 kcal/mol.[21] This difference decreases to 6.7 kcal/mol at the MP-4(SDTQ) level and to 5.6 kcal/mol at the PMP-4 level. Thus, ^{3}1 is close in energy to ^{1}1, but at room temperature the equilibrium constant is only 8.8×10^{-5}, so that at equilibrium there will be about 0.01% of the triplet present in solution at 25 °C. The small amount of triplet may not be readily detected by EPR techniques. The triplet could play a kinetic role if it reacted with lower activation energies than the singlet and if access to this triplet state was not blocked by an activation barrier. Considering the very different geometries of ^{1}1 and ^{3}1, such an activation barrier could be substantial. Use of the correlated MP-2 geometries leads to very small changes in ΔE (^{1}1 – ^{3}1).[22] Substitution of the amino groups to form 3 leads to pronounced changes in the singlet–triplet splitting. The splitting for 3 increases by a factor of ~2.3 to 13.9 kcal/mol at the PUMP-4(SDTQ) level. Thus, there will be no likelihood of observing the triplet at room temperature for the species 3.

The proton affinity of ^{1}1 is 243.1 kcal/mol at 300 K, obtained by using an electronic energy difference of 249.2 kcal/mol at the MP-4 level and the appropriate corrections,[24] This value is similar to that calculated for the protonation of imidazol-2-ylidene (257.3 kcal/mol).[2b] However, the structure of ^{1}1 does not respond to protonation as would be expected for a carbene. We have previously shown that the structural and electronic relation between a carbene and its corresponding carbenium ion (formed by protonation of the carbene center) provides a useful diagnostic for classifying divalent carbon species.[2b] Protonation of a singlet carbene center is expected to give a decrease in the carbon-substituent bond lengths and an increase in the characteristically small valence angle between the original substituents at carbon. The P–C bond in 2 is longer than that in ^{1}1, and the P–C–Si angle decreases rather than increases. Substitution of the amino groups on phosphorus leads to an increased proton affinity for ^{1}3 (257.0 kcal/mol based on an electronic energy difference of 262.5 kcal/mol at the MP-4(SDTQ) level) over ^{1}1. As with ^{1}1, ^{1}3 similarly does not respond to protonation like a carbene. The P–C bond increases by 7.6 pm in 4 and the Si–C bond increases by 9.9 pm. The bond angle at carbon decreases substantially to 128.4°. The P–N bond distances in 4 decrease by 5.5 and 5.2 pm as compared to those in ^{1}3. This is consistent with the increase in $r_{(P-C)}$ of 7.6 pm predicted for going from ^{1}3 to 4. Thus both cations, 2 and 4, have fairly similar structures, although both the C–Si and C–P bonds shorten slightly by 3.4 and 2.6 pm, respectively, in 4 as compared to 2. Both 2 and 4 resemble an experimental structure determination of a C trimethylsilylated analogue of these cations, $[(CH_3)_2N]_2P-C^+-[Si(CH_3)_3]_2$ ($r_{(P-C)}$ = 162.0 pm, $r_{av(Si-C)}$ = 189.4 pm, $\theta_{av(P-C-Si)}$ = 120.5°).[25]

These data support the best characterization of ground state ^{1}1 and ^{1}3 as multiply bonded λ^5-phosphaacetylenes. There are low-lying triplet methylene states (^{3}1 and ^{3}3) which can best be described as λ^3-phosphinomethylenes. Large structural differences in singlet and triplet states may give rise to a substantial activation barrier between the two sets of species.

(21) It is well-known that triplet calculations at the ROHF or UHF levels incorporate some of the effects of the correlation energy, whereas closed-shell SCF calculations do not. Thus, it is inappropriate to take an energy difference from a closed-shell SCF calculation and an open-shell calculation.

(22) The singlet–triplet splitting for 1 is similar to that calculated for PH$_2$CH of 6.2 kcal/mol at the DZ+P/PMP-4 (SDTQ) level. This calculated value is twice the splitting previously reported for this energy difference at the MP-3 level.[23]

(23) Nguyen, M. T.; McGinn, M. A.; Hegarty, A. F. Inorg. Chem. 1986, 25, 2185.

(24) Dixon, D. A.; Lias, S. G. In Molecular Structure and Energetics; Liebman, J. F., Greenberg, A., Eds.; VCH Publishers: Deerfield Beach, FL, 1987; Vol. 2, Chapter 7, p 269.

(25) (a) Igau, A.; Baceiredo, A.; Grützmacher, H.; Pritzkow, H.; Bertrand, G. J. Am. Chem. Soc. 1989, 111, 6853. (b) While this manuscript was being reviewed, a theoretical investigation of related methylenephosphonium ions by Ahlrichs et al. has appeared: Ehrig, M.; Horn, H.; Kölmel, C.; Ahlrichs, R. J. Am. Chem. Soc. 1991, 113, 3701.

Synthesis, Structure, and Dynamics of a Macrocyclophane

Michael Lofthagen, Raj Chadha, and Jay S. Siegel*

Contribution from the Department of Chemistry, University of California, San Diego, La Jolla, California 92093. Received May 2, 1991

Abstract: The synthesis of the macrocyclophane 6 by intramolecular alkyne trimerization using Vollhardt's catalyst is presented. The construction is composed of one 1,3,5-substituted benzene and one 2,6,10-triaminotrioxatricornan subunit linked by three tetramethylene arms. The crystal structures of 5-tos/6-tos and 6 have been determined. 5-tos/6-tos shows a structure distorted from a helical C_3 symmetric conformation, and 6 shows a structure of C_1 symmetry with a void in the interior. Empirical force field and semiempirical calculations, and conformational analysis by ^{1}H NMR techniques, support a noncollapsed solution structure of 6. Low-temperature ^{1}H NMR of 6 reveals a dynamic behavior consistent with a stepwise flip of pitch of the tetramethylene chains.

Macrocages with physical properties stemming from intricate molecular connectivities require the synthesis and characterization of multiply bridged macrocyclophanes.[1] These macrocages have a greater stereochemical complexity[2] than their toroidal counterparts;[3] control of their structure and elucidation of their stereochemistry pose a substantial challenge.[4]

Synthesis

Synthesis of triply bridged macrocyclophanes has been accomplished from three general approaches: (1) coupling of two

(1) (a) Lehn, J.-M. Angew. Chem. 1988, 27, 91–116. (b) Vögtle, F.; Muller, W. M.; Werner, U.; Losensky, H.-W. Angew. Chem., Int. Ed. Engl. 1987, 26, 901–903. (c) Sheridan, R. E.; Whitlock, H. W., Jr. J. Am. Chem. Soc. 1988, 110, 4071–4073. (d) Canceill, J.; Lacombe, L.; Collet, A. J. Am. Chem. Soc. 1986, 108, 4230–4232. (e) Cram, D. J.; Karbach, S.; Kim, Y. H.; Baczynskyj, L.; Marti, K.; Sampson, R. M.; Kalleymeyn, G. W. J. Am. Chem. Soc. 1988, 110, 2554–2560. (f) Murakami, Y. Top. Curr. Chem. 1983, 115, 107–155.

(2) (a) Franke, J.; Vögtle, F. Angew. Chem., Int. Ed. Engl. 1985, 24, 219–221. (b) Schrage, H.; Franke, J.; Vögtle, F.; Steckhan, E. Angew. Chem., Int. Ed. Engl. 1986, 25, 336–338.

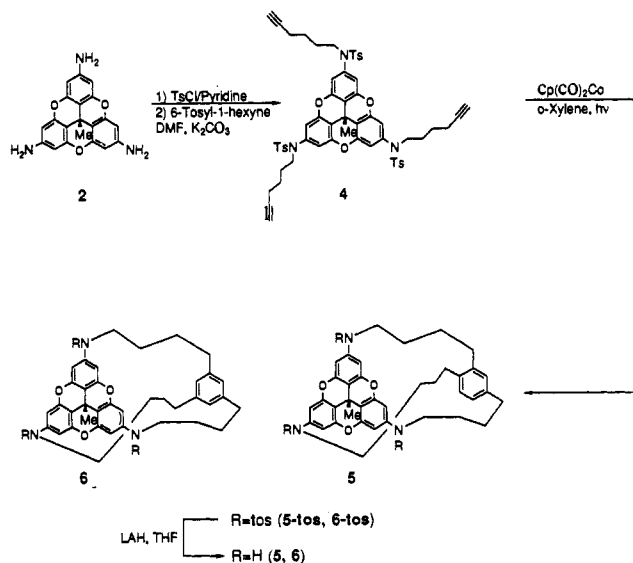(3) Diederich, F. Angew. Chem., Int. Ed. Engl. 1988, 27, 362–386.

(4) Kiggen, W.; Vögtle, F. In Progress in Macrocyclic Chemistry; Izatt, R. M., Christensen, J. J., Eds.; Wiley: New York, 1979; Vol. 3, Chapter 6.
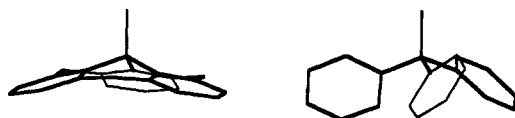
cent-methyltrioxatricornan   1,1,1-triphenylethane

Figure 1. Computer-generated drawings of the X-ray structures of *cent*-methyltrioxatricornan (**1**), oxygens omitted for clarity, and 1,1,1-triphenylethane.

Scheme I

Figure 2. Stereoview projection of the X-ray structure of **6**.

Figure 3. X-ray structure of **6** drawn with 30% probability ellipsoids. View perpendicular to the benzene plane.

keystone units to form all three bridges concomitantly in one pot;[5] (2) first tethering two keystones together and then inducing intramolecular ring closure;[6] and (3) elaborating a single keystone structure with arms ending in units that come together in a subsequent step.[7] At present there are a dearth of examples from the latter class, though the few present are very interesting. We have taken this tack in order to demonstrate its applicability to the development of cage systems in general. Herein we report our findings on a cyclophane composed of one trioxatricornan[8] and one benzene unit.

The starting keystone 2,6,10-triaminotrioxatricornan,[8] **2**, can be viewed as a tris(ortho-bridged) triphenylethane. It is bowl-shaped, with the concave face presenting a large (ca. twice the area of anthracene) smooth surface (Figure 1). This is in contrast to the parent triphenylethane that is viewed as a bowl filled in by its ortho substituents.

The amino groups of **2**, after tosylation, were alkylated with 6-tosyl-1-hexyne in dimethylformamide to give the trialkyne **4**. Intramolecular cyclooligomerization was effected by Vollhardt's catalyst, photoactivated in refluxing xylene (Scheme I).[9] Two regioisomeric, 1,2,4- and 1,3,5-substituted macrocyclophanes **5**-tos/**6**-tos were isolated in 41% yield in a 1:3 ratio.[10]

Attempts to separate the two isomers by multiple crystallization or chromatography failed. The two isomers cocrystallized from several different solvent systems, in some cases yielding crystals

Figure 4. X-ray structure of the **5**-tos/**6**-tos composite. View perpendicular to the benzene plane.

of X-ray quality (vide infra). Evidently, the dominant packing interactions, coming from the trioxatricornan portion of the molecule, allow the incorporation of regiochemical disorder, at the benzene, into the crystal lattice.[11]

Separation of the regio isomers was facilitated by removal of the tosyl groups. Treatment of **5**-tos/**6**-tos with excess lithium aluminum hydride in refluxing THF[12] yielded the mixture **5**/**6** from which pure **6** was isolated by chromatography on silica and/or slow crystallization from benzene/hexanes (Scheme I). Precedence for the oligomerization above is drawn from the intramolecular assembly of simple triply bridged cyclophanes re-

(5) (a) O'Krongly, D.; Denmeade, S. R.; Chiang, M. Y.; Breslow, R. *J. Am. Chem. Soc.* **1985**, *107*, 5544–5545. (b) Hogberg, H.-E.; Wennerstrom, O. *Acta Chem. Scand., Ser. B* **1982**, *B36*, 661–667. (c) Friedrichsen, B. P.; Powell, D. R.; Whitlock, H. W., Jr. *J. Am. Chem. Soc.* **1990**, *112*, 8931–8941.

(6) (a) Haeg, M. E.; Whitlock, B. J.; Whitlock, H. W., Jr. *J. Am. Chem. Soc.* **1989**, *111*, 692–696. (b) Claude, S.; Lehn, J.-M.; Vigneron, J. M. *Tetrahedron Lett.* **1989**, *30*, 941–944.

(7) (a) Bookser, B. C.; Bruice, T. C. *J. Am. Chem. Soc.* **1991**, *113*, 4208–4212. (b) Reference 1d.

(8) Lofthagen, M.; VernonClark, R.; Baldridge, K.; Siegel, J. Submitted for publication.

(9) Vollhart, K. P. C. *Angew. Chem., Int. Ed. Engl.* **1984**, *23*, 539–556.

(10) Only the *out* isomer is possible in this study. For a discussion on *in–out* isomerism, see: Simmons, H. E.; Park, C. H. *J. Am. Chem. Soc.* **1968**, *90*, 2428–2432.
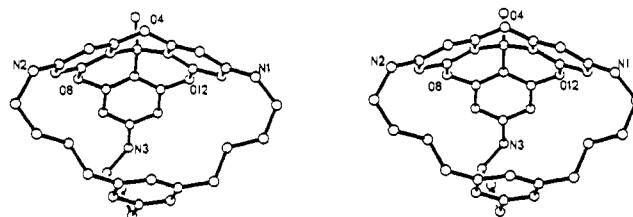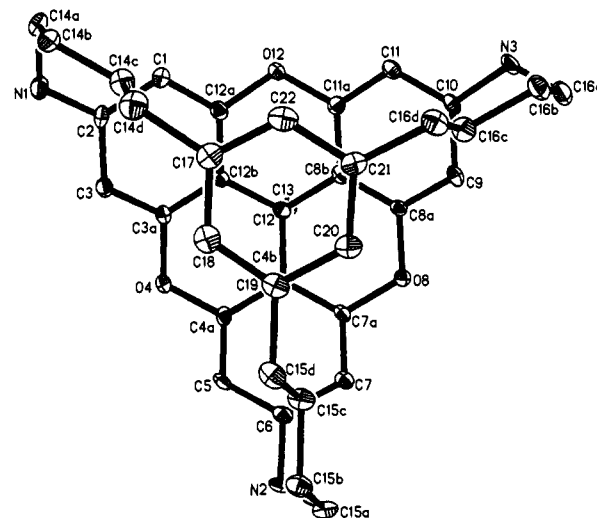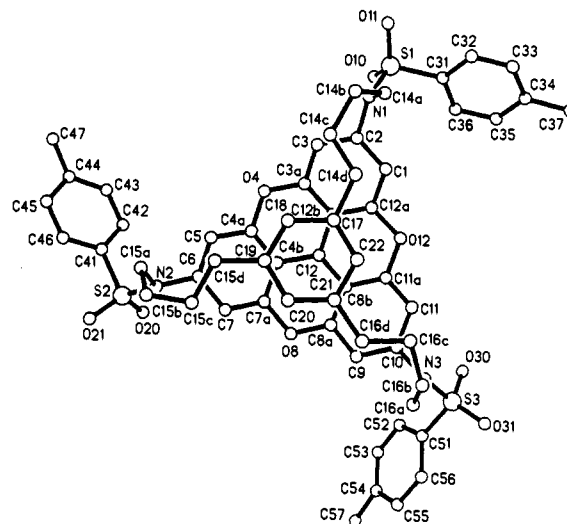
(11) For a discussion of such packing phenomena, see: Weissbuch, I.; Addadi, L.; Berkovitch-Yellin, Z.; Weinstein, S.; Lahav, M.; Leiserowitz, L. *J. Am. Chem. Soc.* **1983**, *105*, 6615–6621.

(12) Fujita, T.; Lehn, J.-M. *Tetrahedron Lett.* **1988**, *29*, 1709–1712.

Synthesis, Structure, and Dynamics of a Macrocyclophane

J. Am. Chem. Soc., Vol. 113, No. 23, 1991 8787

Table I. Symmetry and Void Size of the Cyclophanes **6** and **5**-tos/**6**-tos from the X-ray Structures Compared to EFF- and AM1-Calculated Structures

	X-ray structures		calculated structures					
			EFF			AM1		
	6	**5**-tos/**6**-tos	**6**-I	**6**-II	**6**-III	**6**-I	**6**-II	**6**-III
A^a	4.53	3.82	4.49	4.52	3.44	4.43	4.51	3.78
B	0.07	0.27		0.02		0.02	0.02	0.01
C	0.31	0.28		0.07		0.02	0.04	0.05
ΔE^b			0.0	0.0	+6.0	0.00	+0.01	+4.1

^{a} Key: A, distance from the center of the aromatic ring (1,3,5-benzene) to the best plane of the keystone $(C(Ar)-N)_3$; B, difference between largest and smallest value of the closest distance from the keystone $(C(Ar)-N)_3$ plane to the benzene 1,3,5-carbons; C, difference between largest and smallest value of the distance from the center of the benzene to the closest N on the keystone. ^{b} Calculated relative energies, kcal/mol.

ported by Hubert and Dale.[13] Their system, though elegant by design, led to intractable mixtures of isomers.

Molecular Structure of 5-tos/6-tos and 6

Crystal Structure of 6. Crystals of **6**, $C_{38}H_{39}N_3O_3 \cdot 0.5C_6H_6$, were grown from benzene/hexanes. X-ray data was collected at $-100\ ^\circ C$ and solved in space group $P2_1/n$ with four molecules per unit cell. The solution provided the X-ray structure shown in Figures 2 and 3. The molecules lie in general positions, and their form does not approximate any symmetry higher than C_1; benzene of crystallization fills the interstices among the molecules of **6**.

The two π-systems, the benzene and the trioxatricornan, sit outside of normal van der Waals contact and offer a void in the cyclophane interior.[14,15] The void is too small to accommodate the benzene of crystallization. Examination of the difference Fourier map reveals a negligible amount of residual electron density and cannot account for any occupancy of the void.[16]

Crystal Structure of 5-tos/6-tos. Crystals of **5**-tos/**6**-tos, $C_{59}H_{57}N_3O_9S_3 \cdot C_6H_6$, were grown from benzene/hexanes. X-ray data were collected at room temperature as well as at $-110\ ^\circ C$ and solved in space group $P\bar{1}$ with two molecules per unit cell. The solution provided the X-ray structure shown in Figure 4. Large thermal parameters for the benzene ring and its appendages are seen in the structure. This is likely due to a regioisomeric disorder from the mixture of 1,3,5 and 1,2,4 substitution patterns at the benzene nucleus. Accurate geometric parameters cannot be derived from this structure, but an assessment of the overall molecular conformation is possible.

In this structure, the π-systems are located just outside of van der Waals contacts of one another. The molecule appears to have adopted a twisted geometry that minimizes the void in the structure.

Comparison of Experimental and Computational Geometries

X-ray and Computation. In the X-ray structure of **6**, the alkyl chains connecting the triaminotrioxatricornan to the benzene nucleus are in an extended conformation that forces the two π-systems apart.[17] The chains are disposed in a C_1 manner rather

(13) Hubert and Dale prepared a series of metacyclophanes by the intramolecular trimerization of tris(Ω-alkynyl)benzenes and encountered regiochemical mixtures that were glasses unsuitable for X-ray analysis. See: Hubert, A. J.; Dale, J. *J. Chem. Soc.* **1965**, 3160–3170.

(14) For a discussion on aromatic–aromatic interactions, see: Jorgensen, W. L.; Severance, D. L. *J. Am. Chem. Soc.* **1990**, *112*, 4768–4774.

(15) For a discussion on self-complexation in macrocycles, see: (a) Grootenhuis, P. D. J.; van Eerden, J.; Sudholter, E. J. R.; Reinhoudt, D. N.; Roos, A.; Harkema, S.; Feil, D. *J. Am. Chem. Soc.* **1987**, *109*, 4792–4797. (b) Loncharich, R. J.; Seward, E.; Ferguson, S. B.; Brown, F. K.; Diederich, F.; Houk, K. N. *J. Org. Chem.* **1988**, *53*, 3479–3491. (c) Reference 6a.

(16) For a discussion of water inclusion in aromatic guest–host systems, see: Atwood, J. L.; Hamada, F.; Robinson, K. D.; Orr, G. W.; Vincent, R. L. *Nature* **1991**, *349*, 683–684.

(17) This absence of self-complexation has been observed by Staab and co-workers in both crystal structures and solution studies of a series of [*m*.*n*]-paracyclophanes. See: (a) Staab, H. A.; Dohling, A.; Krieger, C. *Liebigs Ann. Chem.* **1981**, 1052–1064. (b) Bauer, H.; Briaire, J.; Staab, H. A. *Angew. Chem., Int. Ed. Engl.* **1983**, *22*, 334–335.

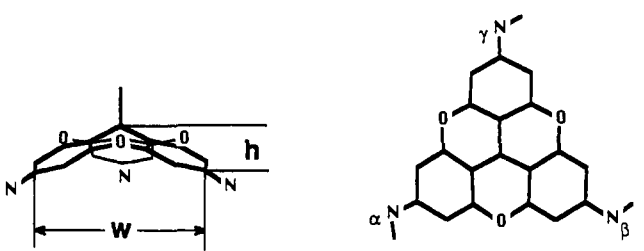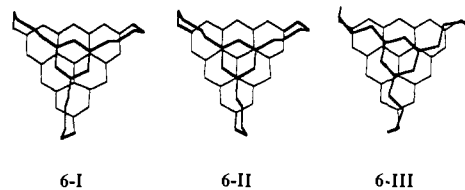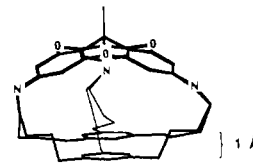6-I   6-II   6-III

Figure 5. Comparison of the EFF-calculated conformers **6**-I, **6**-II, and **6**-III. Oxygen and nitrogen atom labels omitted for clarity. View perpendicular to benzene plane.

6-I/6-III

Figure 6. Composite side-on perspective of the EEF-calculated conformers **6**-I and **6**-III. View in the plane of the benzene ring.

than a more symmetric C_3 structure. The composite structure of **5**-tos/**6**-tos on the other hand is almost of helical C_3 symmetry, and the two π-systems sit closer together (Table I). Thus, from the X-ray results, one can deduce three potentially important conformations of these cyclophanes: open-C3; open-C1; closed-C3.

Empirical force field[18,19] (EFF) and semiempirical AM1[20] calculations were performed to evaluate the conformational preferences for **6**. Three minimum energy structures **6**-I, **6**-II, and **6**-III were obtained by each method; the EFF geometries are shown in Figure 5. The AM1 geometries are extremely close to those found by the EFF method.

6-I and **6**-II differ in the cant of the connecting tetramethylene arms. **6**-I is helical and of C_3 symmetry while **6**-II is C_1, asymmetric; both **6**-I and **6**-II are open forms. **6**-III is the closed structure of C_3 symmetry.

In **6**-I and **6**-II, the keystone portions and dihedral angles of the connecting arms are essentially identical. The EFF-calculated energies for **6**-I and **6**-II differ by less than 0.1 kcal/mol, the AM1 energies by 0.01 kcal/mol.

6-III was obtained by a minimization starting from the crystal geometry of **5**-tos/**6**-tos, in which the tosyl groups had been replaced by hydrogen atoms. This conformation is C_3 symmetric and higher in energy than **6**-I (ca. 6.0 kcal/mol, EFF; 4.1 kcal/mol, AM1).

The composite side-on perspective of **6**-I and **6**-III reveals that **6**-III has a smaller interior void (Figure 6). The distance from the best plane formed by the radial carbons of the keystone, to the center of the 1,3,5-substituted benzene is ca. 1 Å less in the closed form (3.4 Å) than in the open form (4.5 Å). The higher energy of **6**-III is likely due to additional gauche interactions between the β–γ-methylenes in the tetramethylene chains and an unfavorable interaction between the benzene and the β-methylene.[21] The calculations indicate that the open structure, observed in the crystal structure of **6**, results from conformational preferences of the connecting alkyl chains.

The calculated structure **6**-II and the crystal structure of **6** are almost superimposable: The 1,3,5-substituted benzene and the best plane formed by the radial carbons in the keystone are parallel and separated by 4.5 Å. In the crystal structure of **6**, the benzene is slightly displaced from the center of the keystone, probably due to packing forces. Only small differences are seen in the keystone portions and the tetramethylene arms.

(18) EFF calculations were done on PC-MODEL from Serena Software.

(19) Burkert, U.; Allinger, N. L. *Molecular Mechanics*; ACS Monograph Series 177; American Chemical Society: Washington, DC, 1982.

(20) Dewar, M. J. S.; Zoebisch, E. G.; Healy, E. F.; Stewart, J. J. P. *J. Am. Chem. Soc.* **1985**, *107*, 3902–3909.

(21) The higher energy of the conformer **6**-III is approximately equal to the sum of 3 × gauche interactions and 3 × repulsive interaction between the 1,3,5-benzene hydrogens and the β-methylene hydrogens in 1,3,5-triethylbenzene.

Table II. X-ray Geometries and Calculated Structures of the Keystone Portions in **6** and **2**

X-ray Structures

	6-α	6-β	6-γ	2
W		6.80[a]		7.01[a]
h		1.74		1.32
C_q–C_{Me}		1.542 (7)		1.547
oop (keystone)		0.009[a]		0.015[a]
C_{Ar}–N	1.385 (7)	1.410 (6)	1.400 (6)	
C_{Ar}–C_q	1.483 (7)	1.505 (7)	1.499 (7)	1.498[a]
C_{Ar}–C_q–C_{Me}	112.5 (4)	110.0 (4)	111.8 (4)	110.5[a]
C_{Ar}–C_{Ar}–N–$C_δ$	25.5	38.2	43.6	
$\sum$(R–N–R) (deg)	349.5	347.3	344.0	

Calculated Structures

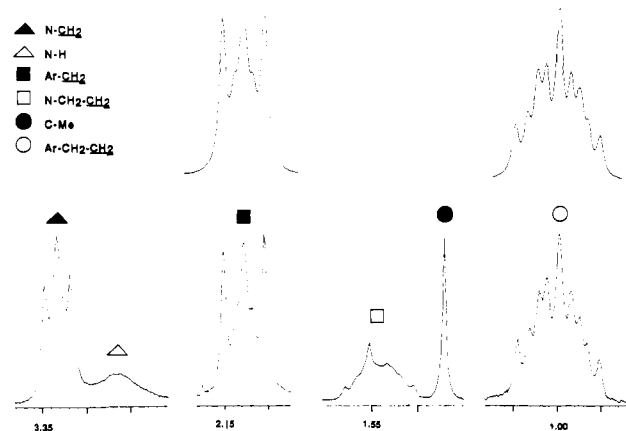|	EFF				AM1			
	6-I	6-II	6-III	2	6-I	6-II	6-III	2
w^a	6.82	6.81	6.83	6.97	6.89	6.80	6.87	7.02
h	1.72	1.75	1.72	1.43	1.68	1.74	1.69	1.35
C_q–C_{Me}	1.53	1.53	1.53	1.53	1.52	1.53	1.50	1.53
C_{Ar}–N^a	1.37	1.37	1.37		1.40	1.40	1.42	
C_{Ar}–$C_q{}^a$	1.50	1.50	1.50	1.50	1.50	1.50	1.50	1.49
C_{Ar}–C_q–$C_{Me}{}^a$	112.6	112.8	112.5	110.7	111.1	110.8	111.1	110.2
C_{Ar}–C_{Ar}–N–$C_δ{}^a$	33	33	39		42	35	58	
$\sum$(R–N–R)^a	360	360	360		344	347	339	

[a] Average value.

The bowl in **6** is more concave than in the parent keystone **2**; the C_{Ar}–C_q–C_{Me} average bond angle is larger in **6** (Table II). It can be argued that this is due to strain imposed by enclosing the trioxatricornan into the cyclophane. However, EFF calculations on the triaminotrioxatricornan alone show the same puckering that is seen in **6-I**. By removing the amines, and reminimizing, the puckering angles decrease. AM1 calculations on the tris-(dimethylamino)-, triamino-, and parent trioxatricornan show the same effect; the molecules with nitrogen in the 2,6,10-positions are more puckered than the parent. Thus, there may be an electronic bias to the strain-induced distortion.

The boatlike distortions (presumably due to packing forces) of the benzene rings seen in **2**,[8] and not observed in **6**, are also responsible for the change in bowl depth. The direction of these boat distortions is such that it leads to a decrease in the bowl depth of **2** as compared to **6**.

The general donor character of the nitrogen atoms is seen in the shorter bond lengths and the less pyramidal nature of the nitrogens compared to normal C(sp²)–N(sp³) single bonds. A more planar nitrogen results in shorter C_{Ar}–N bond length and a smaller C_{Ar}–C_{Ar}–N–$C_δ$ torsion angle, which further supports the idea that the nitrogens are π-bonding with the aromatic ring. A shorter C_{Ar}–N bond length also correlates with a shorter C_{Ar}–C_q bond length and a larger C_{Ar}–C_q–C_{Me} bond angle.

NMR Studies. The solution conformation of the tetramethylene chain in **6** was investigated by using the Karplus relation[22,23] and compared with the structures obtained from the calculations and the X-ray structure (Table III). The methylene portion in the ¹H NMR spectrum in **6** is shown in Figure 7 (lower trace).

The δ-methylene, at 3.4 ppm, appears as a triplet with a coupling constant of 5.2 Hz. Calculations, using a Karplus equation modified for the electronegativity of substituents,[23] indicate that

(22) Karplus, M. *J. Chem. Phys.* **1959**, *30*, 11–15.
(23) Haasnoot, C. A. G.; DeLeeuw, F. A. A. M.; Altona, C. *Tetrahedron* **1980**, *36*, 2783–2792.

Figure 7. Lower trace: observed 360-MHz ¹H NMR spectrum (in CDCl₃) of the aliphatic region in **6**, scale divided into 0.05 ppm increments. Upper trace: simulated spectrum, AA′BB′CC′.

Scheme II
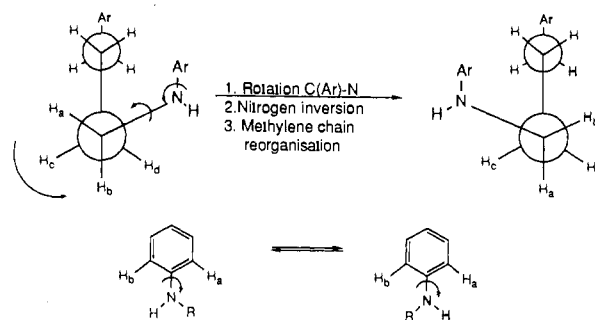
the dihedral angle N–$C_δ$–$C_γ$–$C_β$ is synclinal. However, precise correlations between measured vicinal coupling constants and dihedral angles are hard to make since the $^3J_{HH}$ is not only a function of the dihedral angle.[24]

The α,β,γ-methylene spin systems are complicated by magnetic nonequivalence;[25] the two diastereotopic protons in each methylene are equivalenced by rapid chemical exchange. Six-spin spectral simulation[26] is therefore necessary in order to obtain the coupling constants (Figure 7, upper trace). With the use of the Karplus equation, both the C_{Ar}–$C_α$–$C_β$–$C_γ$ and the $C_α$–$C_β$–$C_γ$–$C_δ$ torsional angles are calculated to be antiperiplanar, ca. 180°, corresponding to the angles expected for the open conformers. For the closed conformer **6-III**, the $C_α$–$C_β$–$C_γ$–$C_δ$ dihedral angle would be synclinal. Thus, in organic solvents the dominant conformer of **6** has an open structure.

Solution ¹H NMR spectra of **6** and **5-tos/6-tos** show a differential anisotropic shift of the proton signals. Johnson and Bovey developed a nomogram,[27] from which, in conjunction with a molecular geometry, one can estimate the chemical shift alteration on a proton induced by the ring current of a proximal benzene ring.

The Δδ for the open (**6-I**) and closed (**6-III**) conformations of **6** were calculated and compared to the observed Δδ for the **6-tos** and **6** protons (Table IV).[28] In both the cyclophanes **6-tos** and

(24) Karplus, M. *J. Am. Chem. Soc.* **1963**, *85*, 2870–2871.
(25) Radcliffe, M. D.; Mislow, K. *J. Org. Chem.* **1984**, *49*, 2058–2059.
(26) NMC SIM Nicolet computer.
(27) Johnson, C. E.; Bovey, F. A. *J. Chem. Phys.* **1958**, *29*, 1012–1014.
(28) The calculated Δδ was obtained as follows: From the EFF-minimized structures **6-I** and **6-III**, the positions of the methylene hydrogens and the benzene (1,3,5) hydrogens relative to the benzene rings of the keystone were expressed in *p* and *z* (according to Johnson et al.[27]). The tabulated upfield shifts could then be obtained.[29] The experimental Δδ was obtained by using suitable model compounds,[30] subtracting the chemical shift of the relevant proton on the model compound from the chemical shift of the anisotropically shifted proton in the cyclophane.
(29) Emsley, J. W.; Feehy, J.; Sutcliffe, L. H. *High resolution Nuclear Magnetic Resonance Spectroscopy*; Pergamon Press: Oxford, 1965; Vol. 1, pp 595–604.
(30) (a) Van Meurs, N. *Recl. Trav. Chim. Pays-Bas* **1967**, *86*, 111. (b) Reference 25.

Synthesis, Structure, and Dynamics of a Macrocyclophane

J. Am. Chem. Soc., Vol. 113, No. 23, 1991 8789

Table III. Dihedral Angles in the Aliphatic Chain of **6**, EFF- and AM1-Calculated and X-ray Structure, Compared to the Dihedral Angles Determined from Measured Solution $^3J_{HH}$ Coupling Constants

	experimental		calculated structures					
			EFF			AM1		
	6 X-ray	^{1}H NMR^a	6-I	6-II	6-III	6-I	6-II	6-III
$C_{Ar}-C_\alpha-C_\beta-C_\gamma$	177	ap (8.2 Hz)	175	178	172	176	177	171
$C_\alpha-C_\beta-C_\gamma-C_\delta$	178	ap (8.5 Hz)	176	177	67	173	176	80
$C_\beta-C_\gamma-C_\delta-N$	62	sc (5.2 Hz)	60	62	54	63	61	66
$C_{Ar}-C_{Ar}-N-C_\delta$	35		33	33	39	42	35	58

^{a} Key: ap, antiperiplanar; sc, synclinal.

Table IV. Calculated Anisotropic Upfield ^{1}H NMR Shifts for the EFF-Minimized Structures **6-I** and **6-III** and Observed Upfield ^{1}H NMR Shifts in **6** and **6-tos**

	$\Delta\delta^a$ (ppm)			
	calculated^b		observed	
	6-I^b	6-III	6-tos	6
$C_{Ar}-H$	0.60	0.89	0.56^c	0.38^c
$C_{Ar}-CH_2-CH_2$	0.40	0.71	0.42–0.52^d	0.34–0.44^d
$C_{Ar}-CH_2-CH_2$	1.11	0.58	0.73–0.83^d	0.52–0.62^d

^{a} Anisotropic upfield ^{1}H NMR shifts. ^{b} Calculated values, based on distance and angle between affected proton and trioxatricornan aromatics.[28] ^{c} Relative to 1,3,5-tripropylbenzene (δ = 6.69 ppm, CDCl$_3$).[30a] ^{d} Relative to hexa-*n*-propylbenzene (lower limit) or *n*-propylbenzene (higher limit).[30b]

6, the β-methylene protons experience the largest upfield shift. This is consistent with the trend seen in the calculated values for $\Delta\delta$ in the open structure **6-I** of the cyclophanes, where the β protons are situated over the keystone aromatic rings. In the closed structure **6-III**, on the other hand, the 1,3,5-substituted benzene protons are expected to experience the largest upfield shift, because of their proximity to the keystone aromatics. The data support a conformation with an open structure in solution.

A rapid exchange process blurs the distinction between the open conformers in the room temperature NMR spectrum (Scheme II). Slowing this exchange process by lowering the temperature allows each conformer to manifest its own spectrum (Figure 8). With use of the Gutowski–Holm approximation,[31] the barrier for the process of equivalencing all exchangeable sites in **6** is estimated at 7.6 kcal/mol. The barrier height indicates that a change of pitch of the three connecting arms does not occur through a synchronous change of all sites, but rather through a stepwise mechanism.[32] The asymmetry of the aromatic peaks in the –130 °C spectrum (motion frozen on the NMR time scale) can be explained by either the exclusive presence of the C_1 conformer or a mixture between the C_1 and the C_3 conformer.

Conclusion

Herein we have demonstrated a novel method for the assembly of three-dimensional host–guest cyclophanes based on the keystone principle combined with an intramolecular cage-closing reaction. The macrocyclophane **6** shows a structure, in solution and solid state, with a void in the interior. The noncollapsed structure is a consequence of the conformational demands of the aliphatic chains that connect the two π-systems. EFF and AM1 calculations predict C_3 and C_1 conformations of **6**, which are roughly equal in energy; the C_1 conformer is found in the X-ray structure of **6**. Variable-temperature ^{1}H NMR studies show that independent motion of the connecting chains is the most likely path for interconversion of these conformers. The low-temperature ^{1}H NMR spectrum is consistent with both isomers being present in solution.

Experimental Section

General Data. Proton NMR spectra were recorded on a ^{1}H NMR spectrometer equipped with a Nicolet 1180E computer interfaced with

(31) Gutowski, H. S.; Holm, C., H. *J. Chem. Phys.* **1956**, *25*, 1228–1234.
(32) The $C_{Ar}-N$ internal rotation in *N*-methylaniline has been measured as 6.9 kcal/mol;[33] a similar value is expected for a single $C_{Ar}-N$ internal rotation in **6**.
(33) Anet, F. A. L.; Ghiaci, M. *J. Am. Chem. Soc.* **1979**, *101*, 6857–6860.
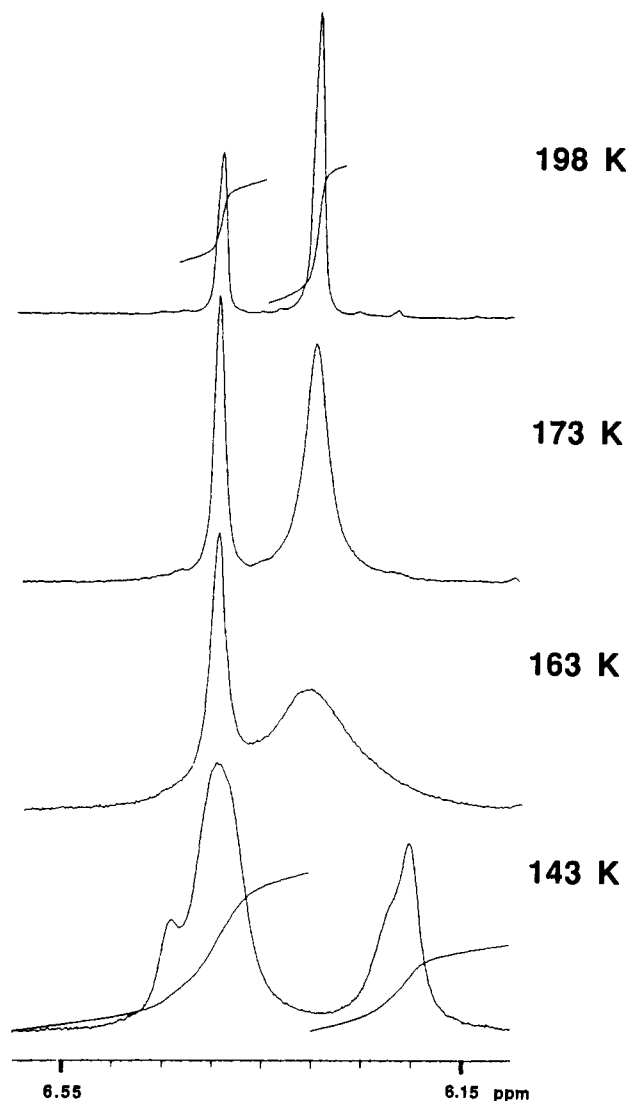

198 K

173 K

163 K

143 K

6.55   6.15 ppm

Figure 8. Variable-temperature 500-MHz ^{1}H NMR spectra of the aromatic region in **6** (in CDCl$_2$F).

an Oxford magnet operating at 360 MHz or on a Varian 500-MHz spectrometer. Carbon NMR were recorded on a QE300 spectrometer operating at 75 MHz carbon or on a Nicolet NT200 spectrometer operating at 50 MHz carbon or on a Varian 500 spectrometer operating at 125 MHz. Infrared spectra were recorded on a Perkin-Elmer 1420 IR spectrometer. UV spectra were recorded on a Perkin-Elmer 6 UV spectrometer. Unless otherwise stated, commercial chemicals were used as supplied.

2,6,10-Tris(tosylamino)-12c-methyl-4,8,12-trioxatricornan (3). 2[8] (1.27 g, 3.68 mmol) was dissolved in 40 mL of pyridine (freshly distilled from KOH). A 2.52-g portion (13.2 mmol) of tosyl chloride was added in portions over 15 min. The solution was refluxed for 1 h, resulting in a pale orange solution. The pyridine was evaporated under reduced pressure. Water (50 mL) was added to the oily residue, and the mixture was sonicated for 30 min. The tan-colored powder was filtered and washed with several portions of water. The powder was dried under vacuum for 2 days, yielding 3.0 g (100%) of **3**: mp 290–295 °C; ^{1}H

NMR (acetone-d_6) δ 9.28 (3 H, s), 7.72 (6 H, d, J = 8.1 Hz), 7.31 (6 H, d, J = 8.1 Hz), 6.86 (6 H, s), 2.34 (9 H, s), 1.30 (3 H, s); ^{13}C{^{1}H} NMR (DMSO-d_6) δ 151.4, 143.6, 138.6, 136.3, 129.9, 126.6, 109.1, 102.5, 31.46, 22.19, 20.90; IR (KBr) 3277, 1626, 1140 cm^{-1}; UV (ETOH) λ_{max} 221 nm (ϵ 77000); FABMS (high resolution) found 808.1425 (calcd for C$_{41}$H$_{34}$O$_9$N$_3$S$_3$ (MH$^+$) 808.1457).

2,6,10-Tris[N-(6-hexynyl)tosylamino]-12c-methyl-4,8,12-trioxatri-cornan (4). 3 (810 mg, 1.0 mmol) was dissolved in 17 mL of dimethylformamide (freshly distilled from calcium hydride). 6-Hexynyl-p-toluenesulfonate (1.52 g, 6.0 mmol) and potassium carbonate (1.66 g, 12.0 mmol) were added. The solution was heated at 75–80 °C for 24 h. The dimethylformamide was then evaporated under reduced pressure, yielding a solid residue. The solid residue was dissolved in THF/diethyl ether and extracted with 0.1 M HCl followed by water. Evaporation of the solvent under reduced pressure yields an oil that solidifies on standing. The crude product was flash chromatographed (silica, 100–200 mesh, 45% ethyl acetate/hexanes) to give 840 mg (80%) of 4. Recrystallization from absolute ethanol yields a white crystalline solid: mp 87–90 °C; ^{1}H NMR (CDCl$_3$) δ 7.55 (6 H, d, J = 8.2 Hz), 7.30 (6 H, d, J = 8.2 Hz), 6.69 (6 H, s), 3.52 (6 H, t, J = 6.0 Hz), 2.46 (9 H, s), 2.20 (6 H, m), 1.89 (3 H, t, J = 2.7 Hz), 1.6–1.55 (15 H, m); ^{13}C{^{1}H} NMR (CDCl$_3$) δ 151.7, 143.8, 139.4, 134.9, 129.6, 127.6, 113.7, 112.5, 83.79, 69.73, 49.88, 31.84, 26.79, 25.02, 24.16, 21.64, 17.78; IR (KBr) 3295, 1615, 1160 cm^{-1}; FABMS (high resolution) found 1048.3369 (calcd for C$_{59}$H$_{58}$N$_3$O$_9$S$_3$ (MH$^+$) 1048.3335). Anal. Calcd for C$_{59}$H$_{57}$N$_3$O$_9$S$_3$: C, 67.60; H, 5.48; N, 4.01. Found: C, 67.87; H, 5.41; N, 3.97.

Tosylcyclophanes 5-tos (1,2,4-Isomer) and 6-tos (1,3,5-Isomer). 4 (580 mg) and CpCo(CO)$_2$ (150 μL) in 30 mL of o-xylene were added via a syringe pump to a solution of CpCo(CO)$_2$ (150 μL) in 400 mL of o-xylene over 18 h. The reaction was irradiated with a 300-W lamp and stirred at reflux during this time. The solvent was then removed under reduced pressure. The crude product was isolated by chromatography on silica (100–200 mesh, 60% hexanes/ethyl acetate). The yield was 240 mg (41%) of an inseparable mixture of 5-tos/6-tos. The 5-tos/6-tos ratio was estimated from ^{1}H NMR integration to be 1:3. In ^{1}H and ^{13}C NMR spectra, only peaks assigned to 6-tos were reported: ^{1}H NMR (CDCl$_3$) δ 7.63 (6 H, d, J = 8.1 Hz), 7.35 (6 H, d, J = 8.1 Hz), 6.62 (6 H, s), 6.12 (3 H, s), 3.53 (6 H, t, J = 5.5 Hz), 2.48 (9 H, s), 2.05 (6 H, t, J = 7.9 Hz), 1.59 (3 H, s), 1.43 (6 H, m), 0.80 (6 H, m); ^{13}C{^{1}H} NMR (CDCl$_3$) δ 152.2, 143.7, 141.2, 140.6, 135.1, 129.6, 127.7, 124.7, 115.3, 113.1, 50.37, 35.79, 30.25, 29.18, 25.18, 21.60; IR (KBr) 1615, 1610, 1165, 665 cm^{-1}; FABMS (high resolution) found 1048.3364 (calcd for C$_{59}$H$_{58}$N$_3$O$_9$S$_3$ 1048.3335). Anal. Calcd for C$_{59}$H$_{57}$N$_3$O$_9$S$_3$: C, 67.60; H, 5.48; N, 4.01. Found: C, 67.77; H, 5.51; N, 4.01.

Cyclophanes 5 (1,2,4-Isomer) and 6 (1,3,5-Isomer). 5-tos/6-tos (45 mg) was dissolved in 5 mL of dry THF. A large excess of lithium aluminum hydride (200 mg) was added, and the solution was refluxed under argon for 72 h. The solution was then cooled with ice, and excess lithium aluminum hydride was quenched by slow addition of 1 mL of water. A 3-mL portion of 1 M sodium hydroxide was added, and the layers were separated. The organic layer was dried with sodium sulfate, and the solvent was removed under reduced pressure. Isolation of pure 6 was achieved by crystallization from benzene/hexanes or by preparative TLC (silica, 1 mm, eluent 60% hexanes/ethyl acetate, R_f = 0.50). Data for 6: mp > 300 °C dec; ^{1}H NMR (CDCl$_3$) δ 6.32 (3 H, s), 6.26 (6 H, s), 3.33 (6 H, t, J = 5.2 Hz), 2.13 (6 H, t, J = 8.2 Hz), 1.56 (6 H, m), 1.47 (3 H, s), 1.00 (6 H, m, J = 8.5 Hz, J = 8.2 Hz); ^{13}C{^{1}H} NMR (CDCl$_3$) δ 153.9, 150.7, 142.3, 124.9, 109.1, 100.2, 46.53, 37.12, 34.82,

31.78, 29.48, 24.80; FABMS (high resolution) found 586.3073 (calcd for C$_{38}$H$_{40}$N$_3$O$_3$ (MH$^+$) 586.3070).

X-ray Crystallography for 6. Crystals of the cyclophane 6 were grown by dissolving 6 in benzene and diffusing hexanes into the solution. A colorless crystal of approximately 0.19 × 0.28 × 0.47 mm was chosen for X-ray measurement. Crystal data: C$_{41}$H$_{42}$N$_3$O$_3$, M = 624.8 g/mol; monoclinic (space group $P2_1/n$); a = 10.429 (3) Å, b = 17.630 (6) Å, c = 18.890 (4) Å, β = 93.69 (2)°; and V = 3466 (2) Å^3, d_{calc} = 1.197 mg/mm^3, Z = 4. X-ray intensities were collected at 173 K on a Siemens R3m/V diffractometer applying Mo Kα radiation (λ = 0.710 73 Å). A total of 5469 independent reflections were collected with 4° < 2θ < 48.0°, of which 2686 with $|F_o|$ > 4$\sigma(F_o)$ were considered unique and observed. The structure was solved by direct methods with the SHELXTL PLUS software. All non-hydrogens were refined anisotropically; hydrogen atoms bonded to the nitrogen were located from a difference Fourier map and refined isotropically. Remaining hydrogen atoms were included at ideal positions with U fixed at 0.08 Å^2. R and R_w factors after refinement of 424 parameters were 0.0585 and 0.0694, respectively. The largest peak in the final Fourier difference map was 0.28 e Å^{-3}.

X-ray Crystallography for 5-tos/6-tos. Crystals of the cyclophanes 5-tos/6-tos were grown by dissolving 5-tos/6-tos in benzene and diffusing hexanes into the solution. A colorless crystal of approximately 0.25 × 0.38 × 0.62 mm was chosen for X-ray measurement. Crystal data: C$_{65}$H$_{63}$N$_3$O$_9$S$_3$, M = 1126.4 g/mol; triclinic (space group $P\bar{1}$); a = 11.363 (3) Å, b = 15.735 (3) Å, c = 16.586 (5) Å, α = 96.37 (2)°, β = 93.69 (2)°, γ = 96.37 (2)°; and V = 2884 (1) Å^3, d_{calc} = 1.297 mg/mm^3, Z = 2. X-ray intensities were collected at 163 K on a Siemens R3m/V diffractometer applying Mo Kα radiation (λ = 0.710 73 Å). A total of 7538 independent reflections were collected with 4° < 2θ < 45.0°, of which 4138 with $|F_o|$ 6$\sigma(F_0)$ were considered unique and observed. The structure was solved by direct methods with the SHELXTL PLUS software. S, N, O, C1–C13, and C31–C57 were refined anisotropically, while disordered carbon atoms (C14–C22 (appended arms and benzene) and C61–C66 (benzene of crystallization)) were refined isotropically. Hydrogen atoms were included at ideal positions with U fixed at 0.08 Å^2. R and R_w factors after refinement of 577 parameters were 0.1054 and 0.1334, respectively. The largest peak in the final Fourier difference map was 1.06 e Å^{-3}.